A cell type-specific cortico-subcortical brain circuit for investigatory and novelty-seeking behavior.

Ahmadlou, M; Houba, J.H.W.; Van Vierbergen, J.F.M.; Giannouli, M.; Gimenez, G.A.; Van Weeghel, C.; Darbanfouladi, M.; Shirazi, M.Y.; Dziubek, J.; Kacem, M.; De Winter, Fred; Heimel, J.A.

published in
Science
2021

document version
Peer reviewed version

A Cell-type Specific Cortico-subcortical Brain Circuit for Investigatory and Novelty Seeking Behavior

Mehran Ahmadlou[1]*, Janou H.W. Houba[1], Jacqueline F.M. van Vierbergen[1], Maria Giannouli[1], Geoffrey-Alexander Gimenez[1], Christiaan van Weeghel[1], Maryam Darbanfouladi[1], Maryam Yasamin Shirazi[1], Julia Dziubek[1], Mejdy Kacem[1], Fred de Winter[2], J. Alexander Heimel[1]*

[1]Cortical Structure and Function Group, Netherlands Institute for Neuroscience, Meibergdreef 47, 1105 BA Amsterdam, The Netherlands.

[2]Laboratory for Neuroregeneration, Netherlands Institute for Neuroscience, Meibergdreef 47, 1105 BA Amsterdam, The Netherlands.

* Corresponding author. E-mail: m.ahmadlou@nin.knaw.nl, a.heimel@nin.knaw.nl

Exploring the physical and social environment is essential for understanding the surrounding world. We do not know how novelty seeking motivation, initiates the complex sequence of actions that make up investigatory behavior. We found in mice that inhibitory neurons in the medial zona incerta (ZIm), a subthalamic brain region, are essential for the decision to investigate an object or a conspecific. These neurons receive excitatory input from the prelimbic cortex to signal the initiation of exploration. This signal is modulated in the ZIm by the level of investigatory motivation. Increased activity in the ZIm instigates deep investigative action by inhibiting the periaqueductal gray region. Interestingly, a subpopulation of inhibitory ZIm neurons expressing tachykinin 1 (TAC1) modulates the investigatory behavior.

One sentence summary

A subpopulation of inhibitory neurons in the zona incerta drives mice to investigate objects and companions.

Investigating the physical and social environment and novelty seeking behavior is essential for finding new food resources, assessing possible dangers and for better understanding of the surrounding world. Novelty seeking behavior can be dissected into the motivational drive, i.e. curiosity, and the investigatory actions. Curiosity, the motivational drive behind this investigating is considered as intrinsic as hunger and thirst (*1*, *2*). Work on neural mechanisms of curiosity focused on centers involved in reward-prediction in tasks with variable, but immediate, rewards (*3*). Curiosity, however, also drives exploration when there is no expectation of immediate reward, as in the case of novelty seeking behavior (*4*). It is unknown which part of the brain drives this novelty seeking behavior. An area that drives approach and reduces fear in the mouse is the zona incerta (*5–10*). Activity in the rostral zona incerta induces eating (*11*), but activity in the medial zona incerta (ZIm) does not induce consummatory behavior and was reported to induce hunting (*7*, *8*). In mice, however, hunting, foraging and object investigation overlap in both their action sequences (approaching, sniffing, grabbing, biting) and in their modulatory sources such as hunger and stress. This has complicated the analysis and interpretation of the experiments investigating these behaviors and consequently understanding the underlying brain circuits. Lacking double choice tests, it was difficult to determine if the ZIm is involved in investigation, and could be essential in novelty seeking behavior.

To investigate a novel object, mice use a different sequence of actions compared to when they interact with a familiar object.

Mice interact with objects in the surrounding environment for different purposes, such as collecting new information to test edibility or hazardousness. Mice interact less with a familiar object compared to a novel object (*12–14*). However, whether the actions taken to investigate a novel object are different from the actions during interaction with familiar objects is not so clear. Using a free-access double choice (FADC) test (**Fig. 1A and movie S1**), we first tested how mice interact with familiar and novel objects.

The number of approaches and duration of all the actions taken to interact, i.e. sniff, carry, grab, and bite were higher in interaction with the novel object than with the familiar object (**Fig. 1A**). An unsupervised Hidden Markov Model (HMM) showed two states of investigatory behavior: 1. approach and sniff without any other interactions and 2. approach and sniff with further interactions with the highest probability to bite (**fig. S1 A**). Further analysis showed that there was also a much higher probability that after sniffing an object, mice continued their investigation by biting when the object was novel compared to when it was familiar, while none of other transitions was significantly different (**Fig. 1B and fig. S1B**). Our data shows that mice, after sniffing, decide to leave the investigation (with sniff to leave probability of 86% and 65% for familiar and novel objects, respectively) or continue the investigation with other sequences of actions, which mostly start with biting (with sniff to bite probability of 9% and 30% for familiar and novel objects, respectively) (**Fig. 1B and fig. S1B**). Therefore, we categorized the object investigation sequences into shallow investigation (where sniffing is not followed by biting) and deep investigation (where sniffing is followed by biting). In both cases, the investigatory event starts with sniff and ends when no investigatory action (i.e. sniff, bite, grab and carry) is taken anymore for at least 100 ms (**fig. S1 C**). We introduced the deep vs. shallow investigation preference (DSP) using the relative time a mouse carries out deep investigation compared to the shallow investigation. DSP varies between $-\pi/2$ and $\pi/2$, where $-\pi/2$ and $\pi/2$ indicate the absolute preference for shallow and deep investigation, respectively, and 0 indicates equal preference for deep and shallow investigation. This depth of investigation was much higher for novel objects than it was for familiar objects (**Fig. 1C**).

GABAergic neurons in ZIm play a key role in object investigation and modulate its depth.

To investigate whether ZIm plays a role in driving object investigation behavior, we expressed ChR2 by AAV to optogenetically activate inhibitory (GAD2+) neurons in the ZIm (**Fig. 1D and fig. S2A**). Activation of the ZIm^{GAD2} neurons in a 2-minute FADC test with a familiar and a novel object showed an

increase in interaction with novel objects (i.e. sniff, bite, grab and carry) and no significant change in interaction with familiar objects (**Fig. 1E, fig. S2B and movie S2**). Activation of the ZIm^{GAD2} neurons in a more complex FADC test, where we put 4 familiar objects and 1 novel object, gave the same results (**fig. S3, A and B and movie S3**). In novel object investigation compared to familiar object investigation, there was a much higher probability of transition from sniffing to biting, while none of other transitions was significantly different (**fig. S2C**), as in the investigatory sequences of actions in wild-type mice. Furthermore, the DSP in novel object interaction under ChR2 activation was much higher than in tdTOM control mice (**Fig. 1F**), implying that there was a higher increase in deep than in shallow investigation.

To further understand whether the observed increased behavior by activation of the ZIm^{GAD2} neurons is investigatory behavior or food-eating and hunting as well, we used an FADC test with one familiarized food pellet and one novel static object and an FADC with one familiarized living cricket and one novel object moving in parallel with the cricket, respectively. Activation of the ZIm inhibitory neurons in both tests resulted in increased interaction with the novel object compared to the food (**Fig. 1G and movie S4**) or the cricket (**Fig. 1H and movie S5**). Moreover, considering movement and shape/odor/flavor as the main components of the cricket that trigger hunting behavior in mice, we used an FADC test with one novel static object and one familiarized moving object and a FADC with one familiarized immobile cricket (dead). Activation of the ZIm^{GAD2} neurons in both tests showed an increase in the novel object interaction (**fig. S4, B and C**), which again shows that the underlying motivation is to investigate and not to hunt. However, in line with results of a previous study (*11*), activation of the inhibitory neurons in the rostral part of the ZI in an FADC test with one familiarized food and one novel object showed an increase in interaction with the food (binge-like eating) compared to the object (**fig. S5**).

To see whether the ZIm inhibitory neurons are essential in object investigation behavior, we used an AAV virus to express stGtACR2 to suppress the ZIm^{GAD2} neurons (**Fig. 1I and fig. S6A**) in a 10-minute

FADC test with a familiar and a novel object. Suppression of the ZIm^{GAD2} neurons showed no significant change in interactions with the familiar objects (**Fig. 1J and movie S6**). However, in interactions with the novel objects, the number of approaches and duration of sniffing, which is a part of both deep and shallow investigation, stayed unchanged while there was a significant decrease in duration of the investigatory actions that are involved in deep investigation (bite, grab and carry) (**Fig. 1J and fig. S6B**). Furthermore, optogenetic deactivation of the ZIm^{GAD2} neurons decreased the transition probability from sniff to bite when the object was novel (**fig. S6C**) and compared to the tdTOM control mice, showed a lower DSP in the novel object investigation (**Fig. 1K**). Deactivation of ZIm^{GAD2} neurons in a familiar open field arena did not cause a significant change in mobility (**fig. S6D**). Chemogenetically silencing ZIm^{GAD2} neurons (by expressing hM4Di in ZIm^{GAD2} and injecting CNO locally in ZIm) showed the same results, i.e. reduction of the investigation duration and the DSP (**fig. S6, E and F**).

GABAergic neurons in ZIm have a major role in social investigation.

We next asked whether ZIm's role in investigation is specific to objects or if it generalizes to conspecifics, where the actions are different from the actions taken in object investigation. To answer this question, first we used tdTOM control mice in a social investigation test, where we introduced a new conspecific (intruder) (**Fig. 2A**). The first and the last third period of the test were considered as novel and familiar periods, respectively (**Fig. 2A**). The significant reduction of the investigation duration in the familiar period compared to the novel period (**Fig. 2A and fig. S7A**) supports the reduction of novelty in the familiar period. An HMM analysis showed two states of investigatory behavior: 1. approach and investigation without grab and 2. approach and investigation with grab (**fig. S8A**). We calculated the transition probability of approach to investigation without grab (AInv) and approach to investigation with grab (AInvG). The AInvG transition probability showed a significant reduction in the familiar period compared to the novel period, while the AInv transition probability did not show a significant difference.

We categorized the social investigation sequences into shallow investigation (where approach is continued by investigation without grab) and deep investigation (where approach is continued by investigation with grab). In both cases, the investigatory event starts with approach and ends when no investigatory action (i.e. anogenital, facial and body sniffing and grabbing) is taken anymore for at least 100 ms (**fig. S8B**). As before we introduced the deep vs. shallow investigation preference (DSP) using the relative time a mouse carries out deep investigation compared to the time spent in shallow investigation. This depth of investigation was much higher in the novel period than in the familiar period (**Fig. 2C**).

Next, we used AAV virus with ChR2 and stGtACR2 to activate and deactivate ZIm^{GAD2} neurons during the social investigation test. Compared to the tdTOM control mice, activation of the ZIm^{GAD2} neurons in a social investigation test showed a substantial increase in duration of the investigatory interaction with the intruder conspecifics, including the approach/chase, anogenital/body/facial investigation, and grabbing and did not induce any aggressive behavior or biting (**Fig. 2D, fig. S7, B and C and movie S7**). Conversely, deactivation of the ZIm^{GAD2} neurons in the social investigation test showed a significant decrease in duration of the investigatory interaction with the intruder conspecific (**Fig. 2D and fig. S7, B and C**). The DSP in the novel period showed the same results as in the novel object investigation (**Fig. 2E**). Chemogenetically silencing ZIm^{GAD2} neurons (by expressing hM4Di in ZIm^{GAD2} and injecting CNO locally in ZIm) showed the same results, i.e. reduction of the investigation duration and the DSP (**fig. S7, D, E and F**).

ZIm is active during investigation and in high arousal state.

To examine whether inhibitory neurons in the ZIm are naturally active during investigatory behavior, we virally expressed GCaMP6s in the ZIm^{GAD2} neurons and recorded calcium photometry signal from freely moving mice during object and social investigation (**Fig. 3A**). In line with the optogenetic results, the calcium photometry showed a significant activity of ZIm^{GAD2} neurons during both deep ($P < 0.0001$) and

shallow ($P < 0.0001$) investigations and a dramatic increase during deep investigation compared to the shallow investigation (**Fig. 3, B and C and fig. S9 A and B**). While in interaction with the food, the same set of actions as the ones in deep investigation, ZIm^{GAD2} neurons show much less activity than deep investigation (**fig. S9 C**).

It is known that investigatory behavior requires a high arousal level (*15*, *16*), which is confirmed by our pupil measurements using head mounted camera in freely moving mice (**fig. S10**). Therefore, we asked whether activity of ZIm neurons is correlated with the arousal level. We recorded from ZIm units in head-fixed mice using a laminar multichannel electrode during spontaneous arousal changes, which were quantified by the changes in pupil size and whisking. 58% of units in the ZIm were significantly correlated with the arousal level (**Fig. 3D**). We optogenetically activated ZIm^{GAD2} neurons in head-fixed mice and video recorded the pupil and whiskers. These measures revealed that activation of the ZIm^{GAD2} neurons increases the arousal level (**Fig. 3E**). Because curiosity-driven investigation has previously been associated with reward anticipation and positive valence (*17*), we examined whether the increased arousal level coincides with a positive or negative valence. We used a real-time place preference/avoidance test in a double-chamber, where one of the chambers is linked to the optogenetic light (light-chamber). Compared to the tdTOM control mice, activation of ZIm^{GAD2} neurons caused an increase in time spent in the light-chamber (**Fig. 3F**). This result was confirmed by the increase of number of returns to the nose poke linked to the photo-activation of the ZIm^{GAD2} neurons in a self-stimulation task (**fig. S11**).

To examine whether the activation of the ZIm^{GAD2} neurons led to a non-specific and general increase in positive arousal and motivation, or if it specifically induced investigatory behavior, we fasted the mice for 24 hours to induce a strong preference for food-eating (familiar food) compared to the novel object investigation (in an FADC test). The control mice (fasted tdTOM mice) showed a strong preference for

the food (**Fig. 3G**), while activation of ZIm^{GAD2} neurons in the fasted mice dramatically increased the novel object investigation and did not affect the food-eating behavior.

Suppressing prelimbic cortex to ZIm pathway reduces investigatory behavior.

Next, we sought the upstream brain areas to the ZIm involved in the investigatory behavior. We injected a monosynaptic Rabies virus (with a previously injected Cre-dependent helper virus) in the ZIm of GAD2-Cre positive mice. Microscopy revealed several brain areas projecting to the ZIm^{GAD2} neurons, among which Prelimbic Cortex (PL) (**Fig. 4A**) is well established in playing a key role in investigatory behavior (*18*, *19*).

Calcium photometry showed that PL→ZIm axons were active during investigation (deep: $P < 0.0001$; shallow: $P < 0.0001$), but there was no significant difference in their activity during deep and shallow investigations (**Fig. 4, B and C**). Moreover, electrophysiological recordings from PL of head-fixed mice showed that activity of 74% of PL units was significantly correlated with the arousal level (**Fig. 4D**). This raised the question whether the increase in arousal level that we had seen by activation of the ZIm^{GAD2} neurons could be inherited from the PL. To answer this, we first injected AAV-ChR2 in PL of C57BL/6 mice under control of a CaMKII excitatory promoter (**fig. S12, A and B**) (**Fig. 4E**). Photo stimulation of the PL→ZIm axons caused an increase in firing rate of ZIm units (**Fig. 4E**) and a significant increase in pupil size and whisking (**Fig. 4F**).

Then we asked whether the direct projection from PL→ZIm is essential for the investigatory behavior. We expressed hM4Di in PL (and tdtTomato as control) and by local injection of CNO in ZIm, we deactivated the PL→ZIm axons in the FADC object investigation and the social investigation tests. This deactivation of PL→ZIm axons significantly reduced the depth of investigation and suppressed object investigation (**Fig. 4G**) and social investigation (**Fig. 4H**). In vivo electrophysiology confirmed the high efficacy of the local injection of CNO in suppressing the PL input into the ZIm (**Fig. 4I**).

These results imply that the PL input into the ZIm contains a motivational signal, which is essential for investigation. At this processing stage the shallow and deep investigations are not differentiated yet by the size of the signal.

ZIm-PAG projection plays a key role in investigation

To determine the investigatory pathway downstream from the ZIm, we first injected a Cre-dependent AAV tdTOM virus in the ZIm of GAD2-Cre positive mice and found projections of the ZIm^{GAD2} neurons to several downstream brain areas, including the Mesencephalic Locomotor Region (MLR), Pontine Reticular Formation (PnO) and Periaqueductal Gray (PAG) (the lateral divisions: lPAG). Using optogenetics and multichannel extracellular recording in head-fixed mice, we examined to what extent activation of the ZIm^{GAD2} neurons affects the neuronal activity in these brain areas. We observed a significant decrease and increase of activity in portions of units in MLR, PnO and lPAG, with the highest effect on suppressing lPAG units (**Fig. 5A**). To find out to which of these brain areas the inhibitory ZIm projection plays a role in the investigatory behavior, we virally expressed ChR2 in ZIm^{GAD2} neurons and optogenetically activated the axon terminals from ZIm into MLR, PnO and lPAG in the FADC object investigation and the social investigation tests. The behavioral results revealed that activation of the ZIm→lPAG projection significantly increased both novel object investigation (**Fig. 5B**) and social investigation (**Fig. 5C**) (compared to the control tdTOM mice) and that activation of the ZIm→MLR and ZIm→PnO did not have an equally strong effect. Activating the ZIm→lPAG axons also increased the depth of investigation (**fig. S13**). Calcium photometry from GCaMP6s expressed in ZIm→lPAG inhibitory axons showed that these axons were active during investigation. However, they were active only during deep investigation ($p = 0.0014$) and not significantly active during shallow investigation ($p = 0.3876$) (**Fig. 5, D and E**). Moreover, in line with our results from activation of the ZIm^{GAD2} neurons, the activation of the ZIm→lPAG (but not ZIm→MLR and ZIm→PnO) inhibitory projection significantly

increased the arousal level (**fig. S14**). To further understand whether this projection is essential for the investigatory behavior, we first virally expressed hM4Di (and tdTomato as control) in the ZIm^{GAD2} neurons. Then, we injected CNO directly into the lPAG to deactivate the ZIm→lPAG inhibitory projection and half an hour later mice went through the FADC object investigation and the social investigation tests. The deactivation of the ZIm→lPAG inhibitory axons significantly reduced the depth and duration of the object investigation (**Fig. 5F**) and social investigation (**Fig. 5G**).

ZIm inhibitory neurons expressing TAC1 are important for investigation

Diversity of the inhibitory subpopulations in the ZI is one of the reasons underlying the functional diversity of the ZI (*7*, *10*, *20*, *21*). Therefore, we sought to identify the inhibitory subpopulations of ZIm and examined their relevance in the investigatory behavior. Because Tachykinin 1 (TAC1) in some thalamic regions (e.g. in the areas where GABAergic neurons originate from the same lineage cells as the ZI, i.e. thalamic reticular nucleus and lateral geniculate nucleus (*22*)) is exclusively expressed in inhibitory neurons (*23*) (https://portal.brain-map.org/), we examined whether TAC1 is also expressed in ZIm inhibitory neurons. Using double fluorescence in situ hybridization (FISH), we found that the vast majority (92%) of TAC1+ neurons in ZIm are inhibitory and they make up for ~11.5% of the inhibitory (VGAT+) neurons (**Fig. 6, A and B**). Furthermore, multi FISH showed that the TAC1+ population is separate from the previously identified Somatostatin positive (SST+) and Parvalbumin positive (PV+) neuronal populations in the ZIm with less than 2% overlap (**Fig. 6, C and D**). This result was confirmed by immunohistochemistry experiments (**fig. S15C**). TAC1+ neurons are more numerous in the medial part of the ZI than in the rostral and caudal parts (**fig. S15, A and B**).

Next, we optogenetically activated these three inhibitory subpopulations to see which inhibitory cell-type in the ZIm is involved in the investigatory behavior. Activation of PV+ neurons and SST+ neurons during the FADC object investigation and the social investigation tests did not cause a significant change in the

investigatory behavior (**Fig. 6, E and F)**. Although we cannot rule out an effect for PV and SST neurons due to the low sample size, activation of the TAC1+ neurons was different and clearly increased both the object and the social investigation (**Fig. 6, E and F**). Activation of the TAC1+ neurons increased the DSP (**Fig. 6G and fig. S16**) and the level of increase in the investigatory behavior by activating the TAC1+ neurons was not different from that induced by activating the GAD2+ neurons (**fig. S17**). Moreover, activation of the TAC1+ neurons increased the arousal level just as activation of GAD2+ neurons did (**fig. S18**).

Next, by optogenetically deactivating the ZIm^{TAC1} neurons during the FADC object investigation and the social investigation tests, we examined whether the ZIm^{TAC1} neurons are essential for the investigatory behavior. Deactivation of the ZIm^{TAC1} neurons suppressed the investigatory behavior (**Fig. 6H and fig. S13, A and B**). Moreover, retrograde AAV injections in the lPAG (and anterograde AAV injections in the ZIm) and Rabies injections in the ZIm of TAC1-Cre positive mice, respectively, showed that ZIm^{TAC1} neurons project to the lPAG (**Fig. 6J and fig. S15E**) and receive direct input from the PL (**Fig. 6K and fig. S15D** for other inputs), which may explain our behavioral results.

Together, our data demonstrates a brain circuit for driving and gating investigatory motivation and novelty seeking behavior. We showed that using a simple approach of free access double choice, we can distinguish investigatory behavior from food-eating and hunting, providing us with a powerful strategy to study brain circuits underlying investigatory behavior. Using this strategy, together with optogenetics, chemogenetics and calcium fiber photometry, we showed that increasing the ZIm activity increases the motivation to investigate. Cortical excitatory input from PL into ZIm conveys non-specific motivation and arousal level to investigate. Extra information (e.g. sensory inputs from midbrain) and processing selectively multiplies the resulting activity of ZIm^{GAD2} neurons. Next, a thresholding mechanism operates on a subpopulation of ZIm^{GAD2} neurons (likely to be ZIm^{TAC1} neurons), in such a way that only high ZIm

activity causes an inhibitory signal to the PAG leading to deep investigation (**fig. S19**). Although the inhibition of PAG can lead to action by disinhibition of defensive actions within the PAG (*5*, *24*), we argue that the increased exploration is not due to decreased fear, because we found activation of ZIm^{GAD2} increased arousal level and specifically increased deep investigation. However, how the sensory information and motivational signals in ZIm integrate to increase the investigatory motivation and initiate this deep investigation remains to be uncovered. Moreover, as dorsal and ventral subdivisions of ZIm differ in their connectivity and neurochemical composition (*25*, *26*), a further subdivision of function may be discovered.

Methods Summary

Mice were habituated to the experimental box for several days. The object investigation test was implemented using a familiar and a novel object in an FADC manner and for social investigation test mice were exposed to one novel conspecific and the test period was split into the first third and the last third as novel and familiar periods for further analysis. Mice were either wild type with no stimulation or they were optogenetically or chemogenetically stimulated or inhibited during the tests (with the corresponding control groups). HMM and transition probability analyses of the labeled behaviors categorized the investigatory behaviors to shallow and deep investigations and investigation duration and depth of investigation were calculated.

Optogenetic effects on arousal level was measured by pupil size and whisker activity. Anatomical and functional connectivity between ZIm and its inputs and outputs was studied using anterograde and retrograde viruses and in-vivo electrophysiology. Calcium activity of ZIm and its input (PL→ZIm axons) and output (ZIm→lPAG axons) was measured during object and social investigation using fiber photometry. Immunohistochemistry and single-molecule mRNA multi-fluoresent in-situ hybridization was performed to examine ZIm^{TAC1} neurons are a subpopulation of ZIm inhibitory neurons. Furthermore,

we photo-activated and photo-inhibited the ZIm^{TAC1} neurons during object and social investigation tests and measured the effects on investigation duration and depth of investigation.

References and Notes:

1. C. D. Spielberger, L. M. Starr, in *Motivation: Theory and research*, H. F. O'Neill, M. Drillings, Eds. (1994), pp. 221–243.

2. G. Loewenstein, The psychology of curiosity: a review and reinterpretation. *Psychol. Bull.* **116**, 75–98 (1994).

3. C. Kidd, B. Y. Hayden, The Psychology and Neuroscience of Curiosity. *Neuron*. **88**, 449–460 (2015).

4. R. N. Hughes, Neotic preferences in laboratory rodents: Issues, assessment and substrates. *Neurosci. Biobehav. Rev.* **31**, 441–464 (2007).

5. X. L. Chou, X. Wang, Z. G. Zhang, L. Shen, B. Zingg, J. Huang, W. Zhong, L. Mesik, L. I. Zhang, H. W. Tao, Inhibitory gain modulation of defense behaviors by zona incerta. *Nat. Commun.* **9**, 1–12 (2018).

6. M. Zhou, Z. Liu, M. D. Melin, Y. H. Ng, W. Xu, T. C. Südhof, A central amygdala to zona incerta projection is required for acquisition and remote recall of conditioned fear memory. *Nat. Neurosci.* **21**, 1515–1519 (2018).

7. Z. D. Zhao, Z. Chen, X. Xiang, M. Hu, H. Xie, X. Jia, F. Cai, Y. Cui, Z. Chen, L. Qian, J. Liu, C. Shang, Y. Yang, X. Ni, W. Sun, J. Hu, P. Cao, H. Li, W. L. Shen, Zona incerta GABAergic neurons integrate prey-related sensory signals and induce an appetitive drive to promote hunting. *Nat. Neurosci.* **22**, 921–932 (2019).

8. C. Shang, A. Liu, D. Li, Z. Xie, Z. Chen, M. Huang, Y. Li, Y. Wang, W. L. Shen, P. Cao, A subcortical excitatory circuit for sensory-triggered predatory hunting in mice. *Nat. Neurosci.* **22**, 909–920 (2019).

9. A. Venkataraman, N. Brody, P. Reddi, J. Guo, D. G. Rainnie, B. G. Dias, Modulation of fear generalization by the zona incerta. *Proc. Natl. Acad. Sci. U. S. A.* **116**, 9072–9077 (2019).

10. X. Wang, X. Chou, B. Peng, L. Shen, J. J. Huang, L. I. Zhang, H. W. Tao, A cross-modality enhancement of defensive flight via parvalbumin neurons in zonal incerta. *Elife*. **8**, 1–17 (2019).

11. X. Zhang, A. N. Van Den Pol, Rapid binge-like eating and body weight gain driven by zona incerta GABA neuron activation. *Science (80-.).* **356**, 853–859 (2017).

12. E. Dere, J. P. Huston, M. A. De Souza Silva, The pharmacology, neuroanatomy and neurogenetics of one-trial object recognition in rodents. *Neurosci. Biobehav. Rev.* **31**, 673–704 (2007).

13. M. Antunes, G. Biala, The novel object recognition memory: Neurobiology, test procedure, and its modifications. *Cogn. Process.* **13**, 93–110 (2012).

14. A. Ennaceur, J. Delacour, A new one-trial test for neurobiological studies of memory in rats. 1: Behavioral data. *Behav. Brain Res.* **31**, 47–59 (1988).

15. D. E. Berlyne, Curiosity and exploration. *Science (80-.).* **153**, 25–33 (1966).

16. M. T. Bardo, R. L. Donohew, N. G. Harrington, Psychobiology of novelty seeking and drug seeking behavior. *Behav. Brain Res.* **77**, 23–43 (1996).

17. M. J. Kang, M. Hsu, I. M. Krajbich, G. Loewenstein, S. M. McClure, J. T. Y. Wang, C. F. Camerer, The wick in the candle of learning: Epistemic curiosity activates reward circuitry and enhances memory. *Psychol. Sci.* **20**, 963–973 (2009).

18. M. Murugan, H. J. Jang, M. Park, E. M. Miller, J. Cox, J. P. Taliaferro, N. F. Parker, V. Bhave, H. Hur, Y. Liang, A. R. Nectow, J. W. Pillow, I. B. Witten, Combined Social and Spatial Coding in a Descending Projection from the Prefrontal Cortex. *Cell*. **171**, 1663-1677.e16 (2017).

19. B. Liang, L. Zhang, G. Barbera, W. Fang, J. Zhang, X. Chen, R. Chen, Y. Li, D. T. Lin, Distinct and Dynamic ON and OFF Neural Ensembles in the Prefrontal Cortex Code Social Exploration. *Neuron*. **100**, 700-714.e9 (2018).

20. C. Kolmac, J. Mitrofanis, Distribution of various neurochemicals within the zona incerta: An immunocytochemical and histochemical study. *Anat. Embryol. (Berl).* **199**, 265–280 (1999).

21. K. Liu, J. Kim, D. W. Kim, Y. S. Zhang, H. Bao, M. Denaxa, S. A. Lim, E. Kim, C. Liu, I. R. Wickersham, V. Pachinis, S. Hattar, J. Song, S. P. Brown, S. Blackshaw, Lhx6-positive GABA-releasing neurons of the zona incerta promote sleep. *Nature*. **548**, 582–587 (2017).

22. N. Inamura, K. Ono, H. Takebayashi, B. Zalc, K. Ikenaka, Olig2 lineage cells generate gabaergic neurons in the prethalamic nuclei, including the zona incerta, ventral lateral geniculate nucleus and reticular thalamic nucleus. *Dev. Neurosci.* **33**, 118–129 (2011).

23. Y. Li, V. G. Lopez-Huerta, X. Adiconis, K. Levandowski, S. Choi, S. K. Simmons, M. A. Arias-Garcia, B. Guo, A. Y. Yao, T. R. Blosser, R. D. Wimmer, T. Aida, A. Atamian, T. Naik, X. Sun, D. Bi, D. Malhotra, C. C. Hession, R. Shema, M. Gomes, T. Li, E. Hwang, A. Krol, M. Kowalczyk, J. Peça, G. Pan, M. M. Halassa, J. Z. Levin, Z. Fu, G. Feng, Distinct subnetworks of the thalamic reticular nucleus. *Nature*. **583**, 819–824 (2020).

24. P. Tovote, M. S. Esposito, P. Botta, F. Chaudun, J. P. Fadok, M. Markovic, S. B. E. Wolff, C. Ramakrishnan, L. Fenno, K. Deisseroth, C. Herry, S. Arber, A. Lüthi, Midbrain circuits for defensive behaviour. *Nature*. **534**, 206–212 (2016).

25. J. Mitrofanis, Some certainty for the “zone of uncertainty”? Exploring the function of the zona incerta. *Neuroscience*. **130**, 1–15 (2005).

26. C. A. Romanowski, I. J. Mitchell, A. R. Crossman, The organisation of the efferent projections of the zona incerta. *J. Anat.* **143**, 75–95 (1985).

27. A. Heimel, Herseninstituut/Ahmadlou_etal_Science_2021. Zenodo (2021). doi:10.5281/zenodo.4588941

28. H. Taniguchi, M. He, P. Wu, S. Kim, R. Paik, K. Sugino, D. Kvitsani, Y. Fu, J. Lu, Y. Lin, G. Miyoshi, Y. Shima, G. Fishell, S. B. Nelson, Z. J. Huang, A Resource of Cre Driver Lines for Genetic Targeting of GABAergic Neurons in Cerebral Cortex. *Neuron*. **71**, 995–1013 (2011).

29. S. Hippenmeyer, E. Vrieseling, M. Sigrist, T. Portmann, C. Laengle, D. R. Ladle, S. Arber, A developmental switch in the response of DRG neurons to ETS transcription factor signaling. *PLoS Biol.* **3**, 0878–0890 (2005).

30. J. A. Harris, K. E. Hirokawa, S. A. Sorensen, H. Gu, M. Mills, L. L. Ng, P. Bohn, M. Mortrud, B. Ouellette, J. Kidney, K. A. Smith, C. Dang, S. Sunkin, A. Bernard, S. W. Oh, L. Madisen, H. Zeng, Anatomical characterization of Cre driver mice for neural circuit mapping and manipulation. *Front. Neural Circuits*. **8**, 1–16 (2014).

31. J. Mattis, K. M. Tye, E. A. Ferenczi, C. Ramakrishnan, D. J. O'Shea, R. Prakash, L. A. Gunaydin, M. Hyun, L. E. Fenno, V. Gradinaru, O. Yizhar, K. Deisseroth, Principles for applying optogenetic tools derived from direct comparative analysis of microbial opsins. *Nat. Methods.* **9**, 159–172 (2011).

32. N. C. Klapoetke, Y. Murata, S. S. Kim, S. R. Pulver, A. Birdsey-Benson, Y. K. Cho, T. K. Morimoto, A. S. Chuong, E. J. Carpenter, Z. Tian, J. Wang, Y. Xie, Z. Yan, Y. Zhang, B. Y. Chow, B.

Surek, M. Melkonian, V. Jayaraman, M. Constantine-Paton, G. K. Wong, E. S. Boyden, Independent optical excitation of distinct neural populations. *Nat. Methods*, **11**, 338–346 (2014)

33. M. Mahn, L. Gibor, P. Patil, K. Cohen-Kashi Malina, S. Oring, Y. Printz, R. Levy, I. Lampl, O. Yizhar, High-efficiency optogenetic silencing with soma-targeted anion-conducting channelrhodopsins. *Nat. Commun.* **9** (2018), doi:10.1038/s41467-018-06511-8.

34. T.W. Chen, T. J. Wardill, Y. Sun, S. R. Pulver, S. L. Renninger, A. Baohan, E. R. Schreiter, R. A. Kerr, M. B. Orger, V. Jayaraman, L. L. Looger, K. Svoboda, D. S. Kim, Ultrasensitive fluorescent proteins for imaging neuronal activity. *Nature.* **499**, 295-300 (2013)

35. M. Kabra, A. A. Robie, M. Rivera-Alba, S. Branson, K. Branson, JAABA: Interactive machine learning for automatic annotation of animal behavior. *Nat. Methods*. **10**, 64–67 (2013).

36. M. Ahmadlou, J. A. Heimel, Preference for concentric orientations in the mouse superior colliculus. *Nat. Commun.* **6**, 6773 (2015).

37. J. P. Sommeijer, M. Ahmadlou, M. H. Saiepour, K. Seignette, R. Min, J. A. Heimel, C. N. Levelt, Thalamic inhibition regulates critical-period plasticity in visual cortex and thalamus. *Nat. Neurosci.* **20**, 1716–1721 (2017).

38. S. N. Kadir, D. F. M. Goodman, K. D. Harris, High-dimensional cluster analysis with the masked EM algorithm. *Neural Comput.* **26**, 2379–2394 (2014).

39. M. Ahmadlou, L. S. Zweifel, J. A. Heimel, Functional modulation of primary visual cortex by the superior colliculus in the mouse. *Nat. Commun.* **9**, 3895 (2018).

Acknowledgements

We thank Joris Coppens, Andres de Groot, Ralph Hamelink, Maurice Heemskerk, Sonja Hofer, Helmut Kessels, Martin Oomstee, Stephen Super, John van Veldhuijzen, Marian Verhage, Nanneke van der Wal and Joost Verhaagen. **Funding:** This work was supported by Dr. J.L. Dobberke Foundation. F.d.W. was supported by Onderzoekfonds KNAW-instituten, ronde 2019. **Author contributions:** M.A. conceived the study with input from J.A.H. M.A., J.H.W.H., J.F.M.v.V., M.G., G.-A.G, C.v.W., M.D., M.K., M.Y.S. and J.D. collected and analyzed the data. F.d.W. made viral vectors and helped the in situ hybridization. M.A. and J.A.H. wrote the paper. **Competing interests:** Authors declare no competing interests. **Data and materials availability:** All processed data are available at github.org/herseninstituut/Ahmadlou_etal_Science_2021 and at Zenodo (27). Raw movies and scripts are stored on institutional storage and are available upon request from the authors.

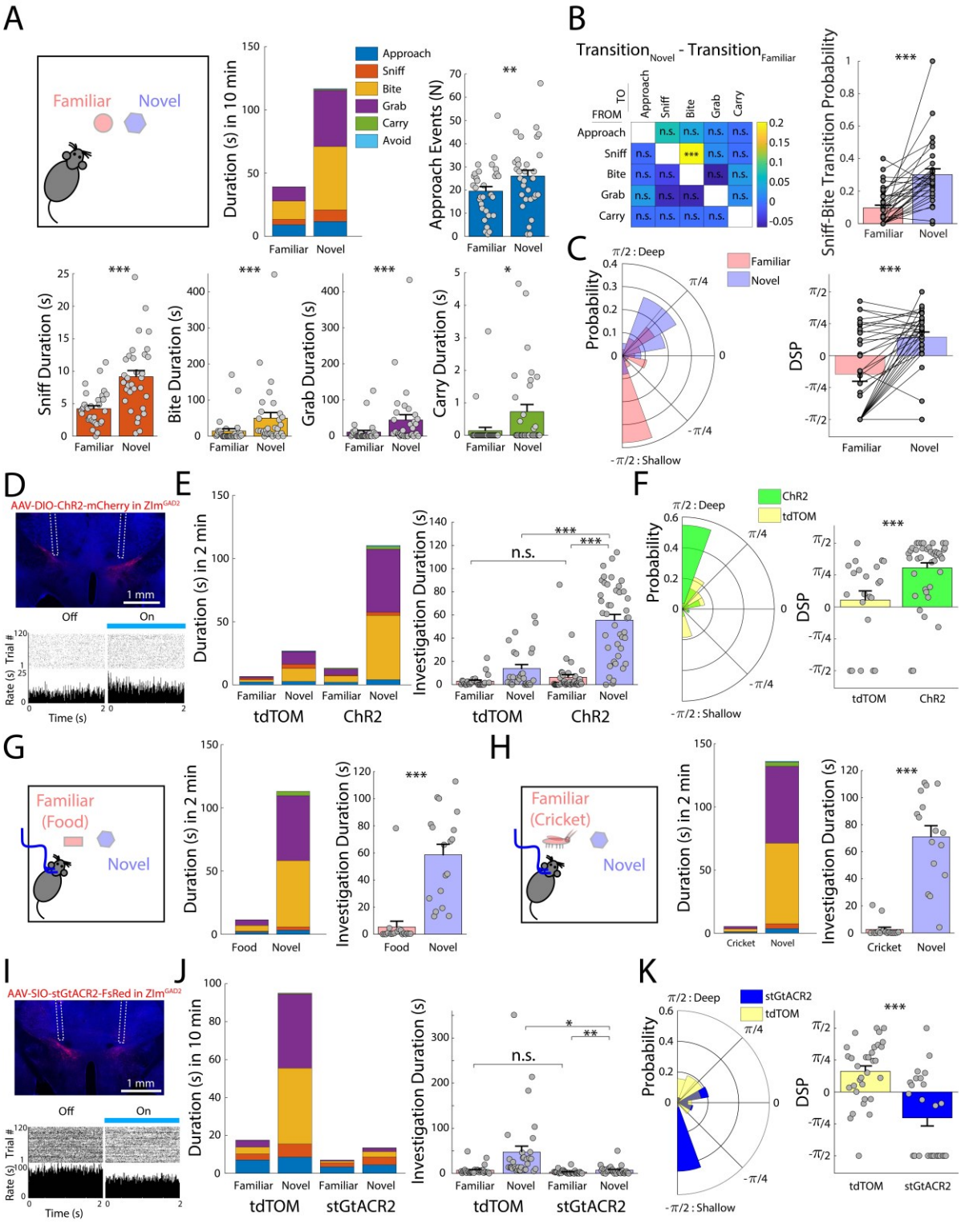
A
Familiar
Novel
Approach
Sniff
Bite
Grab
Carry
Avoid
Duration (s) in 10 min
Approach Events (N)
Sniff Duration (s)
Bite Duration (s)
Grab Duration (s)
Carry Duration (s)
B
Transition Novel - Transition Familiar
TO
FROM
Approach
Sniff
Bite
Grab
Carry
n.s.
Sniff-Bite Transition Probability
C
π/2 : Deep
π/4
0
-π/4
-π/2 : Shallow
Probability
DSP
D
AAV-DIO-ChR2-mCherry in ZIm GAD2
1 mm
Off
On
Trial #
Rate (s)
Time (s)
E
Duration (s) in 2 min
Investigation Duration (s)
tdTOM
ChR2
F
ChR2
tdTOM
G
Familiar (Food)
Novel
Food
H
Familiar (Cricket)
Cricket
I
AAV-SIO-stGtACR2-FsRed in ZIm GAD2
J
stGtACR2
K

Fig 1: Action sequences and role of ZIm GABAergic neurons in object investigation. (**A**) Schematics of an FADC test with familiar and novel objects. Stacked bar graph shows duration for each action (approach, sniff, bite, grab, carry and avoid) taken by C57BL/6 mice to interact with familiar and novel objects averaged over all 10-min tests (n = 37 tests from 8 mice, 4 males). Bar graphs show quantification of individual actions: number of approaches and sniff, carry, grab and bite durations in seconds. (**B**) Representation of the difference between transition matrices of actions taken in novel object and familiar object interactions by the animals in (A). Bar graph shows probability of sniff to bite transition in interaction with familiar and novel objects. (**C**) Probability histogram and bar graph of DSP index of mice in (A) in interaction with familiar and novel objects. DSP varies between $-\pi/2$ and $\pi/2$, where $-\pi/2$ and $\pi/2$ indicate the absolute preference for shallow and deep investigation, respectively, and 0 indicates equal preference for deep and shallow investigation. (**D**) Expression of AAV-ChR2-mCherry in ZIm of a GAD2-Cre mouse and scheme of location of the optic fibers (dashed lines). The lower panel shows an example in-vivo recording of a ZIm neuron with optogenetic light off and on. (**E**) Stacked bar graphs show average duration of actions taken by control mice with tdTomato (n = 27 tests from 4 mice, 2 males) and mice with ChR2-mCherry (n = 42 tests from 7 mice, 4 males) in 2-min FADC tests with familiar and novel objects. Bar graphs show the investigation duration. (**F**) Probability histogram and bar graph of DSP index of mice in (E) in interaction with novel objects. (**G**) Schematics of an FADC test with familiar food and a novel object. The stacked bar graph and the bar graph show duration of the actions and duration of investigation with photoactivation of ZIm^{GAD2} neurons in a 2-min test (n = 16 tests from 7 mice, 4 males). (**H**) Schematics of a FADC with familiar cricket and novel moving object. The stacked bar graph and the bar graph show duration of the actions and duration of investigation with photoactivation of ZIm^{GAD2} neurons in a 2-min test (n = 16 tests from 7 mice, 4 males). (**I**) Example of expression of AAV-stGtACR2-FusionRed in ZIm of a GAD2-Cre mouse and scheme of location of the optic fibers (dashed lines). The lower panel shows an example in-vivo recording of a ZIm neuron with

optogenetic light off and on. (**J**) Stacked bar graphs show average duration of actions taken by control mice with tdTomato (n = 32 tests from 5 mice, 3 males) and mice with stGtACR2-FusionRed (n = 29 tests from 7 mice, 4 males) in 10-min FADC tests with familiar and novel objects. Bar graphs show the investigation duration. (**K**) Probability histogram and bar graph of DSP index of mice in (J) in interaction with novel objects. n.s.: not significant, *: <0.05, **: <0.01 and ***: <0.001.

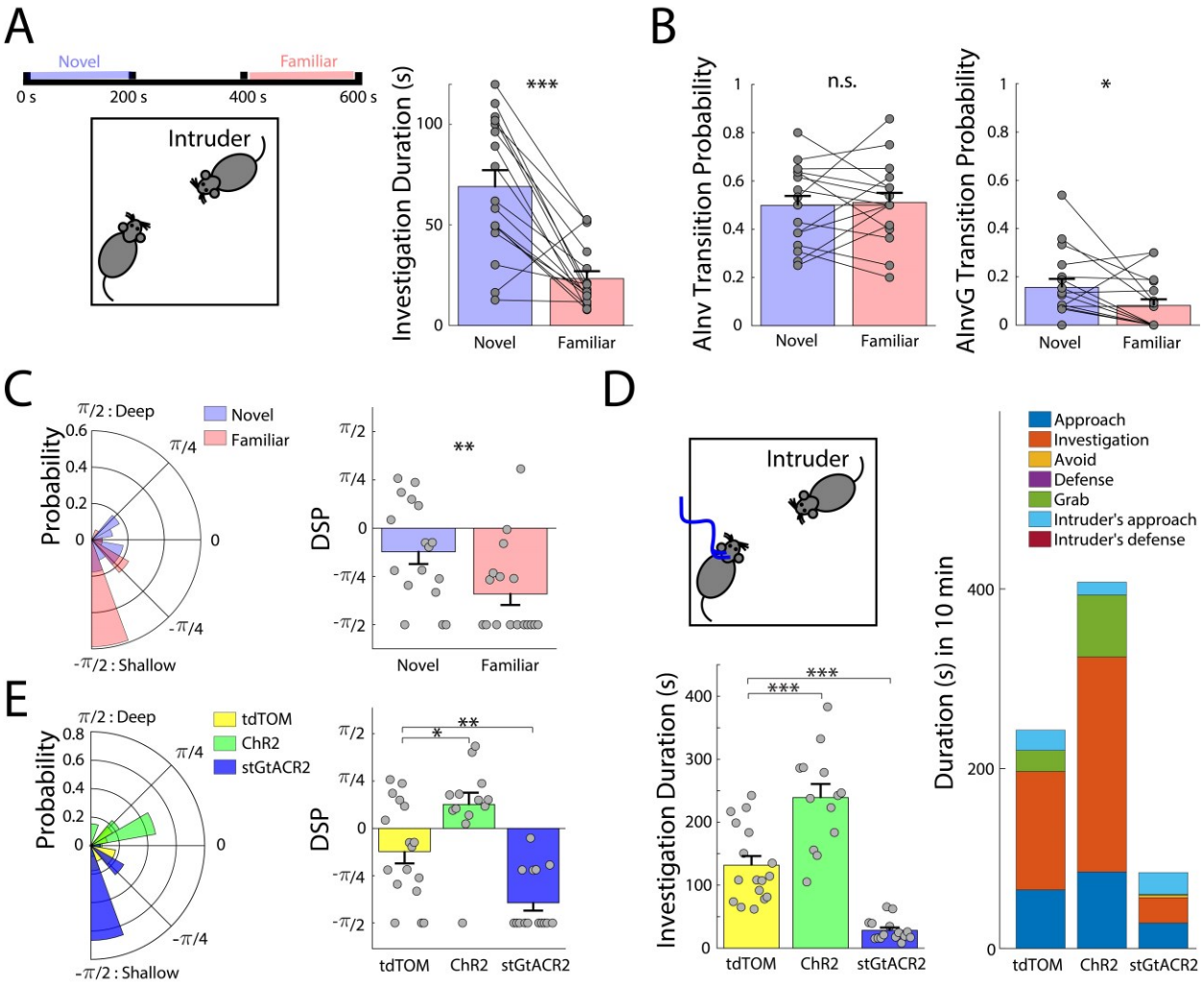

Fig 2: ZIm plays a central role in social investigation. (**A**) Schematics of a 10-min social interaction test, where the first third and the last third of the test are considered novel and familiar periods, respectively. Bar graph shows duration of investigation taken by control tdTomato mice in the familiar and novel periods (n = 17 tests from 8 mice, 4 males). (**B**) Left and right bar graphs show transition from approach to investigation event without grab (AInv) and transition from approach to investigation event with grab (AInvG) in (A), respectively, in the familiar and novel periods. (**C**) Probability histogram and bar graph of DSP index of mice in (A) in familiar and novel periods. (**D**) Schematics shows optogenetic social interaction test. Bar graph shows investigation duration of tdTom (n = 17 tests from 8 mice, 4

males), ChR2 (n = 13 tests from 5 mice, 3 males) and stGtACR2 (n = 15 tests from 6 mice, 3 males) mice in the social interaction test. Stacked bar graph shows duration for each action (approach, investigation, avoid, defense, and grab of the resident mouse, intruder's approach and intruder's defense) taken by the tdTom, ChR2 and stGtACR2 mice. (**E**) Probability histogram and bar graph of DSP index of mice in (D) in the novel period. n.s.: not significant, *: <0.05, **: <0.01 and ***: <0.001.

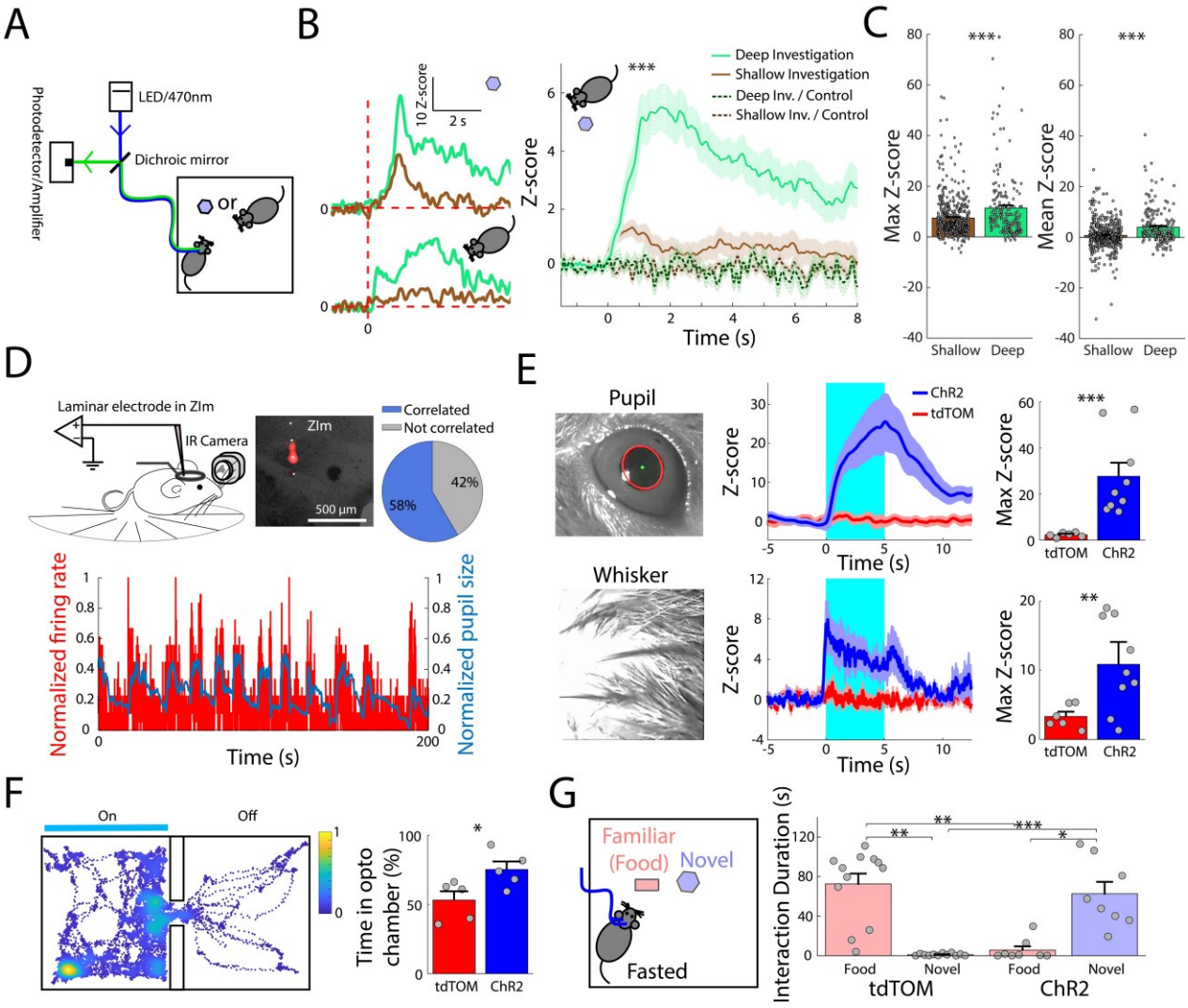

Fig 3: ZIm is active during investigation and in high arousal state. (**A**) Schematics of calcium photometry during social or object interaction. (**B**) Left: Example calcium photometry signals of AAV-GCaMP6s expressing ZIm^{GAD2} neurons during deep (green) and shallow (brown) object investigation (top) and social investigation (bottom). Right: Calcium photometry signals of deep (n = 191 events) and shallow (n = 507 events) investigation averaged over all object and social investigation events (8 mice, 4 males). Signals of control mice with GFP expression in ZIm are represented by dashed lines (n = 58 shallow and deep 91 investigation events from 3 mice, 2 males). Time 0 s indicates start of the

investigation events, i.e. start of sniffing for object investigation and start of approaching the intruder conspecific for social investigation. Dark and the surrounding light colors represent mean±SEM. (**C**) Bar graphs show maximum (left) and mean (right) Z-scores of signals in (B). (**D**) Schematics of extracellular recording of ZIm units with laminar probe and pupil video capturing in awake head-fixed mice. DiI and dashed line show trace of electrode in an example recording from ZIm. Pie diagram shows percentages of the recorded ZIm units that are and are not significantly correlated with the pupil size (n = 173 units from 5 mice, 3 males). Bottom shows normalized pupil size (blue) and normalized firing rate (red) of an example ZIm unit correlated with the pupil size. (**E**) Z-score (middle) and maximum Z-score (right) of pupil size (top) and whisker activity (bottom) of tdTom (red; n = 6 mice, 3 males) and ChR2 (blue; n = 9 mice, 5 males) mice with photo stimulation from 0 to 5 s. (**F**) An example heatmap of the track of a ChR2 mouse in a real time place preference/aversion (RTPPA) test. Bar graph shows duration of time that control tdTom (n = 5 mice, 3 males) and ChR2 (n = 5 mice, 3 males) mice spent in the opto-linked chamber in the RTPPA test. (**G**) Schematics of a fasted mouse in a 2-min FADC test with familiar food and novel object. Bar graph shows duration of time that fasted tdTom (n = 12 tests from 4 mice, 3 males) and fasted ChR2 (n = 8 tests from 6 mice, 4 males) mice interact with the familiar food and the novel object. *: <0.05, **: <0.01 and ***: <0.001.

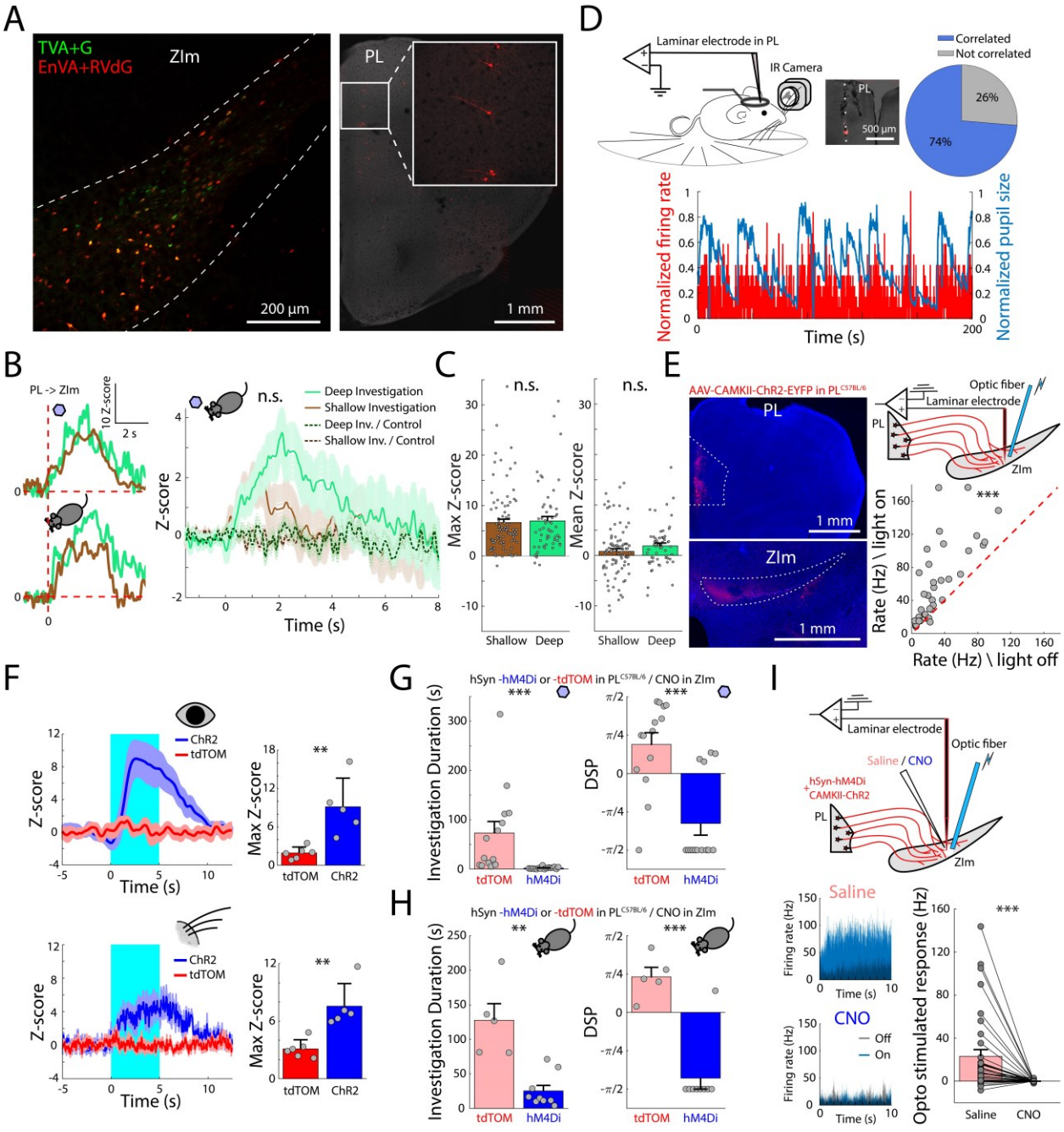

Fig 4: Prelimbic cortex to ZIm pathway is a key factor in investigatory behavior. (**A**) (Left) Retrograde mapping of presynaptic neurons to ZIm^{GAD2} neurons with TVA (GFP) and RVdg (tdTomato). TVA, the avian tumor virus receptor A; G, glycoprotein; EnVA, avian envelope; RVdg, glycoprotein–deleted rabies virus. (Right) Expression of RVdg in ZIm-projecting PL neurons. (**B**) Left: Calcium

photometry signals of PL -> ZIm axons during deep (green) and shallow (brown) object investigation (top) and social investigation (bottom). Right: Calcium photometry signals of deep (n = 57 events) and shallow (n = 90 events) investigation averaged over all object and social investigation events (3 mice, 2 males). Signals of control mice with GFP expression in ZIm are represented by dashed lines. Time 0 s indicates start of the investigation events, i.e. start of sniffing for object investigation and start of approaching the intruder conspecific for social investigation. Dark and the surrounding light colors represent mean±SEM. (**C**) Bar graphs show maximum (left) and mean (right) Z-scores of signals in (B). (**D**) Schematics of extracellular recording of PL units with laminar probe and pupil video capturing in awake head-fixed mice. DiI and dashed line show trace of electrode in an example PL recording. Pie diagram shows percentages of the recorded PL units that are and are not significantly correlated with the pupil size (n = 19 units from 3 mice, 2 males). Bottom shows a normalized pupil size (blue) and normalized firing rate (red) of an example PL unit correlated with the pupil size. (**E**) Left: Expression of AAV-CAMKII-ChR2-EYFP in PL of a C57BL/6 mouse and (Middle) the projections to ZIm. Right: Schematic of in-vivo extracellular recording from ZIm while photo stimulating the PL → ZIm axons (top) and scatter plot of firing rate (Hz) of the ZIm neurons with the optogenetic light above ZIm being on versus off (bottom). (**F**) Z-score (left) and maximum Z-score (right) of pupil size (top) and whisker activity (bottom) of tdTom (red; n = 6 mice, 3 males) and ChR2 (blue; n = 5 mice, 3 males) mice. PL → ZIm axons are photo stimulated from 0 to 5 s. (**G**) Bar graphs show novel object investigation duration (left) and DSP (right) of mice expressing tdTOM (n = 14 tests from 5 mice, 2 males) or hM4Di (n = 16 tests from 5 mice, 2 males) in PL while injecting CNO locally in ZIm. (**H**) Bar graphs show social investigation duration (left) and DSP (right) in the novel period in mice expressing tdTOM (n = 5 tests from 5 mice, 2 males) or hM4Di (n = 9 tests from 5 mice, 2 males) in PL while injecting CNO locally in ZIm. (**I**) Top: schematic of in-vivo extracellular recording from ZIm while photo stimulating the PL → ZIm axons and chemogenetically silencing them by local injection of CNO (top). Bottom left: Firing rate

of an example ZIm neuron in response to photo stimulation of PL → ZIm axons in presence of saline and CNO. Bottom right: bar graph represents responses of ZIm neurons to photo stimulation of PL → ZIm axons in presence of saline and CNO (n = 35 units from 3 mice). n.s.: not significant, *: <0.05, **: <0.01 and ***: <0.001.

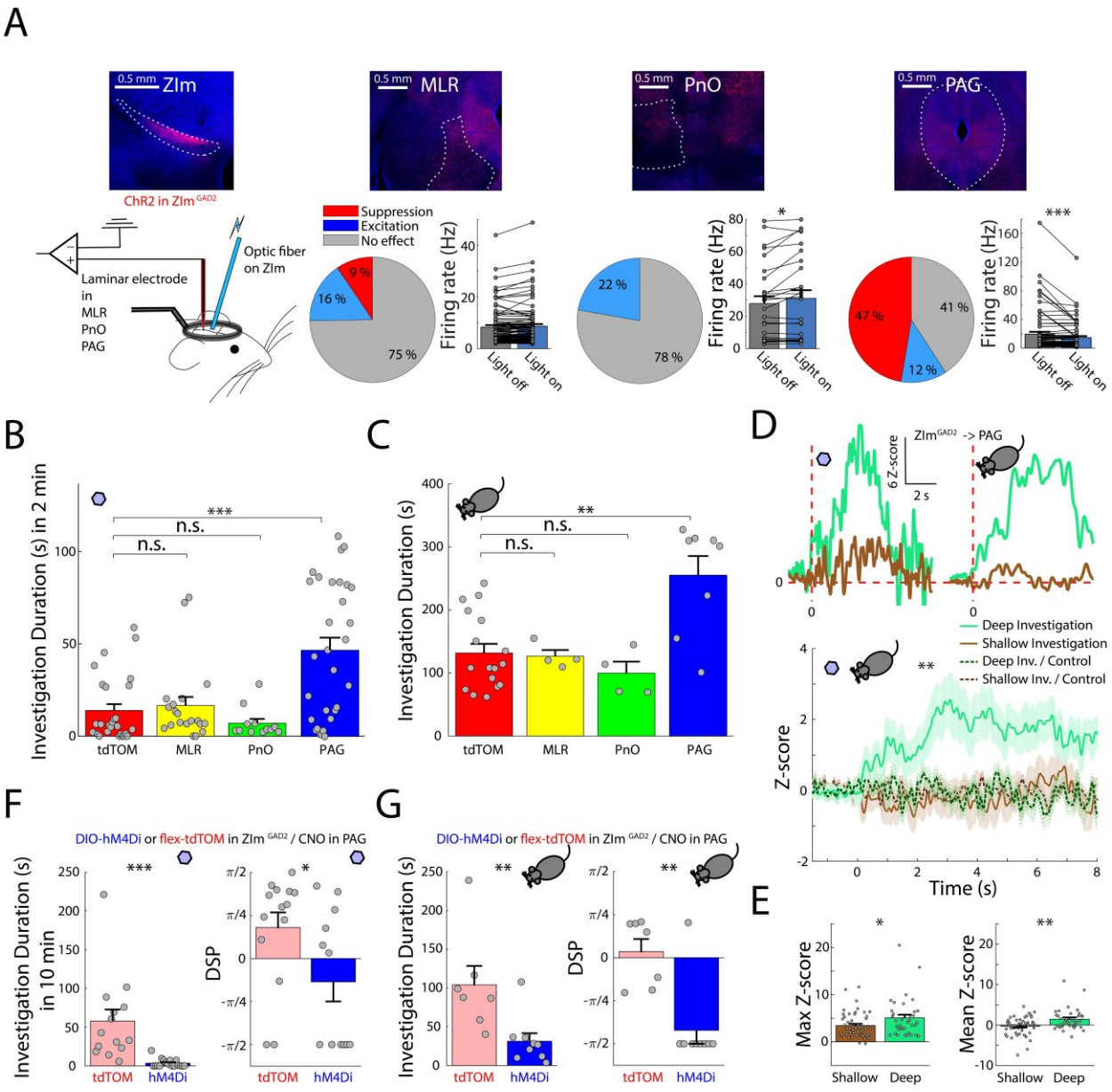

Fig 5: ZIm → PAG projection plays a key role in investigation. (**A**) Expression of AAV-ChR2-mCherry in ZIm^{GAD2} neurons and axons in MLR, PnO and PAG (top; left to right, respectively). The schematics represent the in-vivo experiment of extracellularly recording from ZIm projection targets (MLR, PnO and PAG) while photo stimulating the ZIm^{GAD2}. Pie diagrams show percentage of units in MLR, PnO and PAG (left to right, respectively) that are significantly suppressed (red), excited (blue) or

not changed (gray) by photo stimulation of the ZIm^{GAD2}. Bar graphs show firing rate (Hz) of units in MLR (n = 95 units from 4 mice, 3 males), PnO (n = 27 units from 2 mice, 2 males) and PAG (n = 76 units from 4 mice, 2 males) (left to right, respectively) when photo stimulation light above the ZIm^{GAD2} is off or on. (**B**) Bar graph shows the duration of novel object investigation in control mice with tdTomato (n = 27 tests from 4 mice, 2 males) and mice with ChR2 photo stimulation of ZIm^{GAD2} → MLR (n = 19 tests from 3 mice, 2 males), ZIm^{GAD2} → PnO (n = 12 tests from 3 mice, 2 males) and ZIm^{GAD2} → PAG (n = 30 tests from 5 mice, 3 males) in 2-min FADC tests with familiar and novel objects. (**C**) Bar graph shows the duration of social investigation in control mice with tdTomato (n = 17 tests from 8 mice, 4 males) and mice with ChR2 photo stimulation of ZIm^{GAD2} → MLR (n = 4 tests from 3 mice, 2 males), ZIm^{GAD2} → PnO (n = 4 tests from 3 mice, 2 males) and ZIm^{GAD2} → PAG (n = 8 tests from 5 mice, 3 males). (**D**) Top: example calcium photometry signals of ZIm^{GAD2} → PAG axons during deep (green) and shallow (brown) object investigation (left) and social investigation (right). Bottom: Calcium photometry signals of deep (n = 36 events) and shallow (n = 50 events) investigation averaged over all object and social investigation events (3 mice, 1 male). Signals of control mice with GFP expression in ZIm are represented by dashed lines. Time 0 s indicates the start of the investigation events, i.e. start of sniffing for object investigation and start of approaching the intruder conspecific for social investigation. Dark and the surrounding light colors represent mean±SEM. (**E**) Bar graphs show maximum (left) and mean (right) Z-scores of signals in (D). (**F**) Bar graphs show novel object investigation duration (left) and DSP (right) after injecting CNO locally in PAG of mice expressing tdTOM (n = 14 tests from 5 mice, 3 males) or hM4Di (n = 17 tests from 5 mice, 3 males) in ZIm^{GAD2}. (**G**) Bar graphs show social investigation duration (left) and DSP (right) in the novel period after injecting CNO locally in PAG of mice expressing tdTOM (n = 7 tests from 5 mice, 3 males) or hM4Di (n = 9 tests from 5 mice, 3 males) in ZIm^{GAD2}. n.s.: not significant, *: <0.05, **: <0.01 and ***: <0.001.

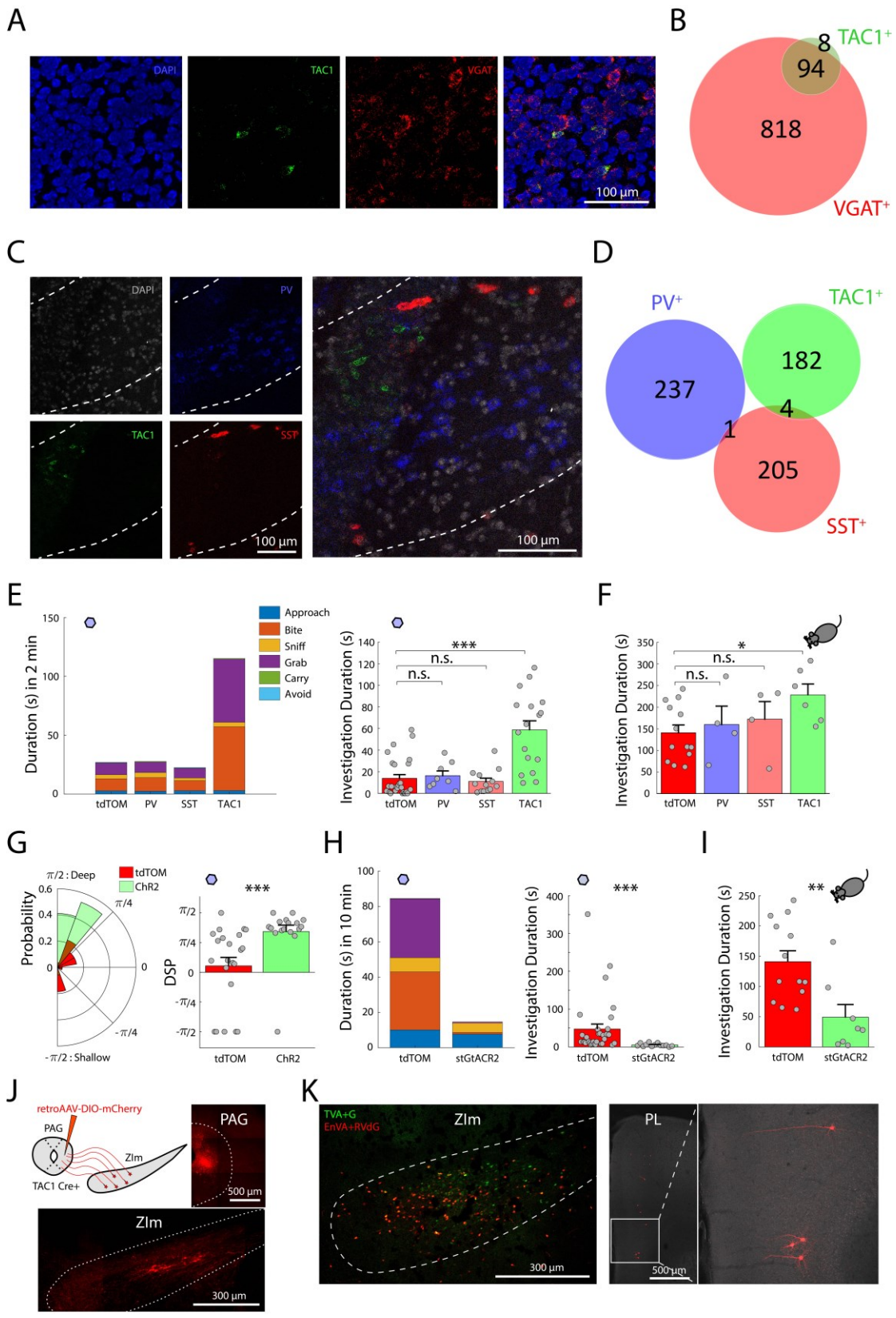
A
DAPI
TAC1
VGAT
100 µm
B
TAC1+
8
94
818
VGAT+
C
DAPI
PV
TAC1
SST
100 µm
100 µm
D
PV+
TAC1+
237
182
4
1
205
SST+
E
Duration (s) in 2 min
Approach
Bite
Sniff
Grab
Carry
Avoid
tdTOM
PV
SST
TAC1
Investigation Duration (s)
***
n.s.
n.s.
F
Investigation Duration (s)
*
n.s.
n.s.
G
π/2 : Deep
tdTOM
ChR2
Probability
-π/2 : Shallow
DSP
***
tdTOM
ChR2
H
Duration (s) in 10 min
tdTOM
stGtACR2
Investigation Duration (s)
***
I
Investigation Duration (s)
**
J
retroAAV-DIO-mCherry
PAG
ZIm
TAC1 Cre+
PAG
500 µm
ZIm
300 µm
K
TVA+G
EnVA+RVdG
ZIm
300 µm
PL
500 µm

Fig 6: The small subpopulation of ZIm inhibitory neurons expressing TAC1 is important for investigation. (**A**) Example of a double-color in-situ mRNA hybridization in ZIm. DAPI is shown in blue and TAC1+ and VGAT+ cells are shown in green and red, respectively. The right shows the overlap between the three colors. (**B**) Venn diagram represents number of TAC1+, VGAT+ and TAC1+/VGAT+ cells in ZIm (from 8 slices). (**C**) Example of a triple-color in-situ mRNA hybridization in ZIm. DAPI is shown in gray and PV+, SST+ and TAC1+ cells are shown in blue, red and green, respectively. The right shows the overlap between the four colors. (**D**) Venn diagram of ZIm cells expressing PV, SST and TAC1 (from 8 slices). (**E**) Stacked bar graphs show average duration of actions taken by control mice with tdTomato (n = 27 tests from 4 mice, 2 males), and mice with ChR2-mCherry expression in ZIm in PV+ neurons (n = 8 tests from 3 mice, 2 males), in SST+ neurons (n = 13 tests from 3 mice, 2 males) and in TAC1+ neurons (n = 17 tests from 5 mice, 3 males) in 2-min FADC tests with familiar and novel objects. Bar graphs represent duration of the novel object investigation. (**F**) Bar graphs represent duration of social investigation in control mice with tdTomato (n = 13 tests from 4 mice, 2 males), and mice with ChR2-mCherry expression in ZIm in PV+ neurons (n = 4 tests from 3 mice, 2 males), in SST+ neurons (n = 4 tests from 3 mice, 2 males) and in TAC1+ neurons (n = 6 tests from 5 mice, 3 males) in social investigation test. (**G**) Probability histogram and bar graph of DSP index of control and TAC1-Cre mice in (E) in interaction with novel objects. (**H**) Stacked bar graph shows average duration of actions taken by control mice with tdTomato (n = 32 tests from 5 mice, 3 males) and mice with stGtACR2-FusionRed expression in ZIm^{TAC1} (n = 13 tests from 5 mice, 3 males) in 10-min FADC tests with familiar and novel objects. Bar graph shows duration of the novel object investigation. (**I**) Bar graph represents duration of social investigation in control mice with tdTomato (n = 13 tests from 4 mice, 2 males) and mice with stGtACR2-FusionRed expression in ZIm^{TAC1} (n = 8 tests from 5 mice, 3 males). (**J**) Schematic of a retrograde tracing experiment with injection of retroAAV-EYFP is PAG of TAC1-Cre mice (n = 2 mice, 2 males) and examples of the EYFP expression in the injection site (PAG) and in the PAG-projecting

ZIm^{TAC1} neurons. (**K**) Left: Rabies monosynaptic retrograde tracing experiment shows the expression of TVA and RVdG in neurons at the injection site (ZIm) in a TAC1-Cre mouse (n = 2 mice, 1 male). Right: expression of RVdG in the PL neurons (right) projecting to ZIm^{TAC1} neurons. n.s.: not significant, *: <0.05, **: <0.01 and ***: <0.001.

List of Supplementary Materials

Materials and Methods

Figs. S1 to S20

Tables S1 to S2

Movies S1 to S7

References only cited in Supplementary Materials (*28–39*).